agronomy

Article

Valorization of *Arbutus unedo* L. Bark Through Chemical Composition Analysis, Liquefaction, and Bio-Based Foam Production

Luísa Cruz-Lopes [1,2,*], Yuliya Dulyanska [1,2], Rogério Lopes [3], Idalina Domingos [1,4], José Ferreira [1,4] and Bruno Esteves [1,4]

1 CERNAS (Centre for Natural Resources, Environment and Society), IPV Research Centre, Polytechnic University of Viseu, Av. Cor. José Maria Vale de Andrade, 3504-510 Viseu, Portugal; ydulyanska@esav.ipv.pt (Y.D.); ijd@estgv.ipv.pt (I.D.); jvf@estgv.ipv.pt (J.F.); bruno@estgv.ipv.pt (B.E.)
2 Department of Environmental Engineering, Polytechnic University of Viseu, Av. Cor. José Maria Vale de Andrade, 3504-510 Viseu, Portugal
3 Department of Mechanical Engineering and Industrial Management, Polytechnic University of Viseu, Av. Cor. José Maria Vale de Andrade, 3504-510 Viseu, Portugal; rogeriolopes@estgv.ipv.pt
4 Department of Wood Engineering, Polytechnic University of Viseu, Av. Cor. José Maria Vale de Andrade, 3504-510 Viseu, Portugal
* Correspondence: lvalente@estgv.ipv.pt

Abstract: *Arbutus unedo* (strawberry tree) is a small Mediterranean tree capable of vigorous regrowth after disturbances like fire. Traditionally used for biomass fuel, its bark and branches hold potential for higher-value products through ecovalorization into liquid mixtures that could replace petroleum-based materials. This study aimed to explore the chemical composition of various components of *Arbutus unedo* and to produce a liquefied material from its internal (IB) and external bark (EB). Chemical compositions of internal and external bark were determined using TAPPI standards including ash, extractive content, lignin, and cellulose. Metal cations were analyzed by ICP. Liquefaction of bark was optimized in a PARR reactor, evaluating factors such as particle size, temperature, and time, and the best polyols were monitored by FTIR-ATR. Polyurethane foams were made with internal and external bark materials liquefied by polymerization with isocyanate, a catalyst, and water as a blowing agent. Results showed that EB has a higher extractive and lignin content, while IB contains more cellulose. Liquefaction yields were higher for IB (74%) than EB (68%), with IB yielding polyols that produced stronger and more resilient foams with higher compressive strength and modulus of elasticity. Mechanical properties of the foams were influenced by the NCO/OH ratio and catalyst levels. Overall, the internal bark demonstrated superior performance for foam production, highlighting its potential as an eco-friendly alternative to petroleum-derived materials.

Keywords: *Arbutus unedo*; liquefaction; polyurethane foam; chemical composition; ecovalorization

Citation: Cruz-Lopes, L.; Dulyanska, Y.; Lopes, R.; Domingos, I.; Ferreira, J.; Esteves, B. Valorization of *Arbutus unedo* L. Bark Through Chemical Composition Analysis, Liquefaction, and Bio-Based Foam Production. *Agronomy* **2024**, *14*, 2893. https://doi.org/10.3390/agronomy14122893

Received: 30 September 2024
Revised: 18 November 2024
Accepted: 26 November 2024
Published: 4 December 2024

1. Introduction

Strawberry tree (*Arbutus unedo*) is one of 122 different species from the genus Arbutus, most common in the American continents and in the Mediterranean region [1]. In the Americas, species include *Arbutus arizonica*, *A. madrensis*, *A. menziesii*, *A. occidentalis*, *A. tessellata*, and *A. xalapensis*. Mediterranean species include *A. unedo*, *A. andrachne*, *A. pavarii*, and *A. canariensis*, along with two hybrids: *Arbutus* × *andrachnoides* (*A. unedo* × *A. andrachne*) and *Arbutus* × *androsterilis* (*A. unedo* × *A. canariensis*) [1]. Strawberry tree is distributed around the Mediterranean, found in western, central, and southern Europe, northeastern Africa, the Canary Islands, and western Asia, and particularly in Portugal, Spain, France, Italy, Albania, Greece, and parts of the former Yugoslavia, as well as some Mediterranean islands [1]. In Portugal, these species have a significant importance since the country is the largest world producer of this fruit [2]. With the increased production of these fruits,

several waste materials are available, one of which is bark. The bark of this tree is grey or red-brownish, and it fissures and peels off in small flakes [3]. It was formerly used in tanning due to the high amount of tannins [4], but it is not used anymore.

There is not much information about the chemical composition of *Arbutus unedo* bark, but it is probably similar to the bark of other species of the same genus. As stated in Dönmez [5], the bark of *Arbutus andrachne*, a tree from the same genus as *Arbutus unedo*, yielded 0.3% hexane extract, 10.1% acetone/water, and 22.4% water extractives. Fatty acids and sterols were the primary components in the lipophilic extractive samples, and fatty acids made up 32.03%, with palmitic acid being the most abundant. Sitosterol was the only phytosterol detected. Two phenolic compounds, 3,4-dihydroxybenzoic acid and catechin, were also identified. Additionally, some mono- and disaccharide sugars, along with their alcohol derivatives, were detected [5]. In this study, the total amount of suberin monomers was 11.36 mg/g in *A. andrachne,* which corresponds to about 1.1% [5]. Another study involving *Arbutus xalapensis* determined the water extract (10.7%), of which 5.7% was made up of condensed tannins [6].

Bark liquefaction using polyalcohols is an emerging process in the valorization of biomass, specifically woody by-products, such as tree bark [7–9]. As a renewable and underutilized resource, bark contains a variety of organic compounds, including lignin, cellulose, hemicellulose, and in some cases, suberin, which can be chemically transformed into valuable products. Liquefaction is a thermochemical process that involves breaking down the complex structures of lignocellulosic materials under moderate heat and pressure conditions, using polyalcohols (e.g., glycerol, ethylene glycol) as solvents or reagents. These polyalcohols act as reactive agents that promote depolymerization and facilitate the conversion of lignocellulosic biopolymers into liquid intermediates. The resulting bio-based liquids have applications in multiple industries, including adhesives [10,11], resins [12], and polyurethane foams [13,14], replacing or complementing petroleum-derived chemicals. This approach supports sustainability goals by converting lignocellulosic waste into high-value products, reducing dependency on fossil fuels, and enhancing the economic potential of forest-based industries. Mainly, two types of catalysts are used: acid and basic. Acid catalysts are the most used because they help in the hydrolysis of the complex structures of lignin, cellulose, and hemicellulose in bark or other lignocellulosic materials. Sulfuric acid is probably the most used acid catalyst, but different acids have been used, for instance, p-Toluenesulfonic acid for the liquefaction of *E. globulus* bark [7], or acetic, lactic, and citric acids to liquefy Kraft lignin [15]. Basic catalysts like sodium hydroxide have also been used, especially in cork-rich barks like *Quercus suber* [16] or *Pseudotsuga menziesii* [17]. Cellulose is predominantly hydrolyzed into glucose [18], while hemicelluloses are broken down primarily into their monomeric sugar components. Lignin, in contrast, undergoes depolymerization and solubilization when exposed to an acidic medium and polyhydric alcohols [19,20]. Initially, lignin is depolymerized into smaller phenolic fragments, which are subsequently esterified with glycerol and ethylene glycol to improve their solubility. Together, these processes degrade the lignocellulosic structure of wood, producing a liquefied mixture composed of various organic compounds.

Foams produced from liquefied wood and bark represent an innovative and sustainable alternative to conventional petroleum-based foams, such as polyurethane. By combining these liquefied components with isocyanate and suitable catalysts and blowing agents, lightweight foams can be produced for applications in packaging, insulation, and cushioning [21–23]. Liquefied lignocellulosic materials only substitute the petroleum-based polyol, but some attempts have been made in order to substitute isocyanate with a less toxic chemical in the so-called non-isocyanate polyurethanes (NIPUs) [24–26].

In this work, the chemical composition of the internal and external bark of *A. unedo* was determined, and its influence on the liquefaction process and on the resulting polyurethane foams was studied.

2. Materials and Methods

The reagents used for polyol synthesis included glycerol (Sigma-Aldrich, St. Louis, MO, USA, ≥99.5%), ethylene glycol (≥99.8%, Sigma-Aldrich, St. Louis, MO, USA,), sulfuric acid (analytical grade, Merck, Darmstadt, Germany), methanol (A.C.S. grade, ≥99.8%, Fisher Chemical, Fair Lawn, NJ, USA), ethanol (analytical grade, absolute, >99.8%, Fisher Chemical, Fair Lawn, NJ, USA),), and ultrapure water (produced in-house). For foam production, di-n-butyltin dilaurate (95%, Sigma-Aldrich, St. Louis, MO, USA) was used as catalyst, along with the surfactant Tegostab B8404®® (Evonik, Essen, Germany), isocyanate MDI Voranate M229®® (average functionality of 2.7, %NCO 31.1%, Dow, Midland, MI, USA), and ultrapure water (produced in-house).

2.1. Chemical Composition

The chemical composition of IB and EB was analyzed by determining their ash content, extractives (in dichloromethane, ethanol, and hot water), cellulose, lignin, and hemicelluloses. The average composition of both samples was assessed using a particle size fraction between 0.420 mm and 0.250 mm.

The ash content was determined by calcifying the material at 525 °C, following the standardized method outlined in Tappi T 211 om-93 [27].

Extractives were quantified through Soxhlet extraction, using 3 g of each sample and 200 mL of solvent. The extraction was carried out sequentially, starting with dichloromethane (DCM), followed by ethanol and hot water, progressing from less to more polar solvents. The procedure adhered to Tappi T 204 standards [28] for wood and pulp extractives. The extraction times were 6 h for DCM and 16 h for both ethanol and hot water. The content of extractives was expressed relative to the dry mass of the samples.

The determination of insoluble lignin was performed using a modified Klason method, according to TAPPI T 222 om-02 [29]. In this procedure, 350 mg of sample was treated with 3 mL of 72% sulfuric acid at 30 °C for 1 h, while stirring every 10 min. Subsequently, 84 mL of distilled water was added, and the mixture was transferred to 100 mL thermal glass bottles and autoclaved at 120 °C for 1 h. After cooling in an ice bath, the samples were filtered using crucibles with pore sizes of 5–15 µm, dried, and weighed. The lignin content was expressed as a percentage of the dry wood.

Cellulose content was measured following the Kürschner and Höffer procedure [30], involving four sequential reflux treatments of grape stalks using a nitric acid and ethanol mixture (1:4, v/v) for 1 h per treatment.

Hemicellulose content was calculated by difference.

2.2. Sample Liquefaction

Arbutus unedo L. (strawberry tree) Internal bark (IB) and External bark (EB) samples were oven-dried at 100 °C and finely ground to increase surface area. A 10 g portion of the dried sample was weighed and placed into a reactor. A 50:50 mixture of glycerol and ethylene glycol, along with 3% sulfuric acid (based on sample weight), was then added. The mixture completely submerged the wood sample, and the reactor (Parr 5100 Series High-Pressure Reactor (Parr Instrument Company, Moline, IL, USA) with a 600 mL capacity) was sealed to prevent leakage. Stirring at 75 rpm was initiated to ensure homogeneous mixing. Three temperatures (140 °C, 160 °C, and 180 °C) with 60 min reaction times were used, and three different times (15 min, 30 min, and 60 min) at 180 °C were also tested. In each test, the temperature was gradually raised to the desired temperature and maintained for the chosen time. These conditions have been used since they obtained good results before [31]. Afterward, the reactor was allowed to cool to room temperature, and the liquefied product was recovered. The resulting material was dissolved in 100 mL of methanol and filtered for further use. Liquefaction yield was determined as follows:

$$\text{Liquefaction yield } (\%) = \left(1 - \frac{\text{Solid residue (g)}}{\text{Dry bark (g)}}\right) \times 100 \quad (1)$$

All liquefactions were performed in triplicate.

2.3. Foam Preparation

The polyol with the best liquefaction yield (180 °C, 60 min) was used to manufacture the foams. The methanol was removed in a rotary evaporator. Afterwards, the polyol was neutralized with NaOH, removing the remaining water with a rotary evaporator followed by 24 h at 100 °C. To prepare the foam, 4 g of neutralized and dried polyol was placed in a polypropylene container. Isocyanate was added in measured amounts using a syringe to insert it into a cylindrical container (dimensions: 60 × 120 mm). The surfactant was then introduced to control the foam bubble size and distribution. Water was added as a blowing agent to react with the isocyanate, generating carbon dioxide for foam expansion. The mixture was mixed at 2000 rpm for 1–2 min, ensuring uniformity. Subsequently, the catalyst (DBTDL) was introduced to speed up the reaction between polyol and isocyanate, promoting foam formation. Additional mixing followed at 2000 rpm for another 1–2 min, during which foam began to rise. It was allowed to expand freely under ambient conditions. Standard proportions used included 4 g polyol, 0.4 g water (10%), 0.28 g surfactant (7%), 0.24 g catalyst (6%), and 10.5 g isocyanate, with variations in water (5–20%), catalyst (3–10%), and isocyanate index (0.6–1).

2.4. Foam Testing

The prepared polyurethane foam was shaped into a cylindrical sample (approximately 60 mm in diameter and 30 mm in height) for compression testing. The sample was placed between the compression plates, and the testing parameters were configured, including a compression speed of 5 mm/min. The Universal Test Machine Servosis I-405/5 was used to apply a gradual and consistent compression force to the foam, while the applied force and corresponding deformation were recorded in real time. Compression continued until the foam underwent significant deformation, stabilizing when most of the foam was compressed.

The mechanical properties were evaluated following the ISO 844 [32] standard with some modifications. Cylindrical slices of PU foam were positioned in the machine and subjected to an increasing compressive load. Each test was conducted in triplicate.

For most foams, there was no failure. Therefore, the compressive stress at 10% deformation (σ_{10}) was used and determined by the following equation:

$$\sigma_{10} = \frac{F_{10}}{A_0} \times 1000\ (\text{kPa}) \quad (2)$$

where F_{10} represents the applied force corresponding to 10% deformation of the sample (N), A_0 denotes the base area of the cylindrical specimen (mm^2). Equation (3) presents the calculations made to determine Young's modulus.

$$\textit{Young's modulus} = \frac{\Delta F/\Delta x \times h_0}{A_0} \times 1000\ (\text{kPa}) \quad (3)$$

where $\Delta F/\Delta x$ is the slope of the linear zone of the stress vs. deformation curve (N/mm^2), and h_0 is the average height of the cylindrical specimen (mm).

2.5. FTIR Analysis

The foam samples were dried in an oven at 102 ± 2 °C overnight, followed by grinding in a mortar. The FTIR spectra were collected using a Perkin Elmer UATR Two FT-IR Spectrometer (Beaconsfield, UK) with a resolution of 4.0 cm^{-1} and 72 scans recorded over the range of 4000–400 cm^{-1}. Powder samples were placed directly onto the crystal to fully cover its surface, with three spectra taken for each sample.

3. Results and Discussion

The strawberry tree bark was divided into IB and EB. Their chemical composition was determined and is presented in Table 1.

Table 1. Chemical composition of internal and external strawberry tree bark.

	Internal Bark (IB)	External Bark (EB)
Ashes	7.57	10.21
Ethanol extractives	8.63	8.64
Dichloromethane extractives	2.39	4.27
Hot Water extractives	9.14	10.00
Klason Lignin	31.52	44.25
Cellulose	26.35	22.99
Hemicelluloses	21.98	9.84

Extractives were determined sequentially by extraction with dichloromethane, ethanol, and water. Dichloromethane extractives are mainly various lipophilic compounds such as terpenes, resins, fatty acids, sterols, waxes, and certain essential oils. A study conducted with *Arbutus andrachne* bark found that the lipophilic extractives were mainly composed of fatty acids and sterols, with palmitic acid being the most prevalent; therefore, it is expected that *Arbutus unedo* bark also has mainly fatty acids. There is a higher content of lipophilic extractives in EB, with around 4.3% compared to 2.4%, both higher than the hexane extract from *Arbutus andrachne* bark [5]. Ethanol extractives represent the second most important extractive in strawberry tree, with approximately 8.6% for each type of bark. Water extracts represent a major extract in both barks, just slightly higher than ethanol extractives. Nevertheless, some of the extractives that could be removed by water were already removed with ethanol; therefore, if the water extraction was conducted first, it would probably have a higher content. Overall, EB had a higher percentage of extractives (22.9%) than the IB (20.2%). The main difference between EB and IB was in their lignin content, with EB containing a significantly higher proportion (44%) compared to IB, which had 32%. On the contrary, polysaccharides had a higher content in IB with about 26% cellulose and 22% hemicelluloses. EB might have a small amount of suberin, about 1%, as determined for *Arbutus andrachne* [5].

Figure 1 shows the liquefaction yield of both IB and EB at three different temperatures. The data provide insights into the effect of temperature on the efficiency of the liquefaction process for both types of bark.

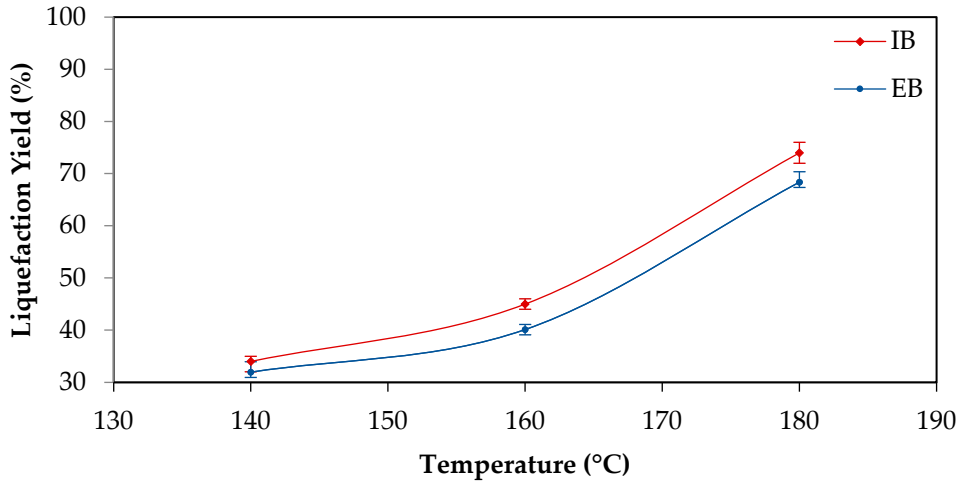

Figure 1. Liquefaction yields at different temperatures for the IB and EB (constant parameters: time 60 min and ratio bark: solvent of 1:10).

As shown in the figure, the liquefaction yield increases with rising temperature for both IB and EB. At 140 °C, the yield is relatively low, around 30%, but it significantly improves at higher temperatures, reaching approximately 70–80% at 180 °C. This trend confirms the anticipated positive correlation between temperature and liquefaction efficiency. Furthermore, under the same conditions, IB exhibits a slightly higher yield compared to EB. This difference is likely attributable to the less condensed structure of IB, which facilitates easier liquefaction.

Similar variation is seen for different liquefaction times with liquefaction yield increasing from around 30% at 15 min to 80% at 60 min, Figure 2. Similar results were obtained before by several other lignocellulosic materials, for example, wood [33], fruit shells [34] or barks [17], although for cork-rich barks with higher suberin content, the liquefaction was made with a basic catalyst. In some cases, a decrease in liquefaction yield is observed for higher temperatures and longer liquefaction times due to polycondensation reactions, which was not the case here. Generally, polycondensation reactions are due to the reactions between polysaccharides and lignin derivatives and usually happen when higher-weight polyols such as PEG are used [35]. The use of low-weight polyols can significantly reduce polycondensation reactions, which has been attributed to highly polar hydroxyl groups with shot chains creating highly protic solvents [8]. The liquefaction yield of both internal (74%) and external (68%) bark was higher than that obtained for eucalyptus bark (62%) at similar conditions [9].

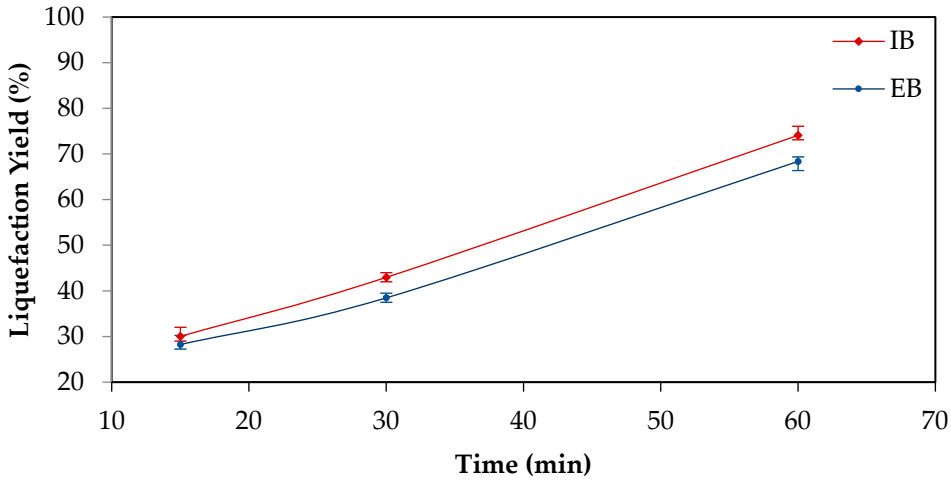

Figure 2. Liquefaction yields at different times for the IB and EB (constant parameters: temperature 180 °C and ratio bark: solvent of 1:10).

The chemical changes with the liquefaction were monitored by FTIR analysis that was done on both the liquefied materials (Figures 3 and 4) and the solid residues after liquefaction (Figures 5 and 6).

The main difference observed between the initial IB and EB spectra is the high absorption observed at 1600 cm^{-1} in the IB (Figures 4 and 6). This high absorption is usually attributed to higher lignin content that has a strong absorption at 1600 cm^{-1} due to the abundance of aromatic C=C bonds. Nevertheless, in this case it is probably due to the overall higher absorption in IB, since there is also a higher absorption around 3330 cm^{-1} and 1030 cm^{-1} in initial IB.

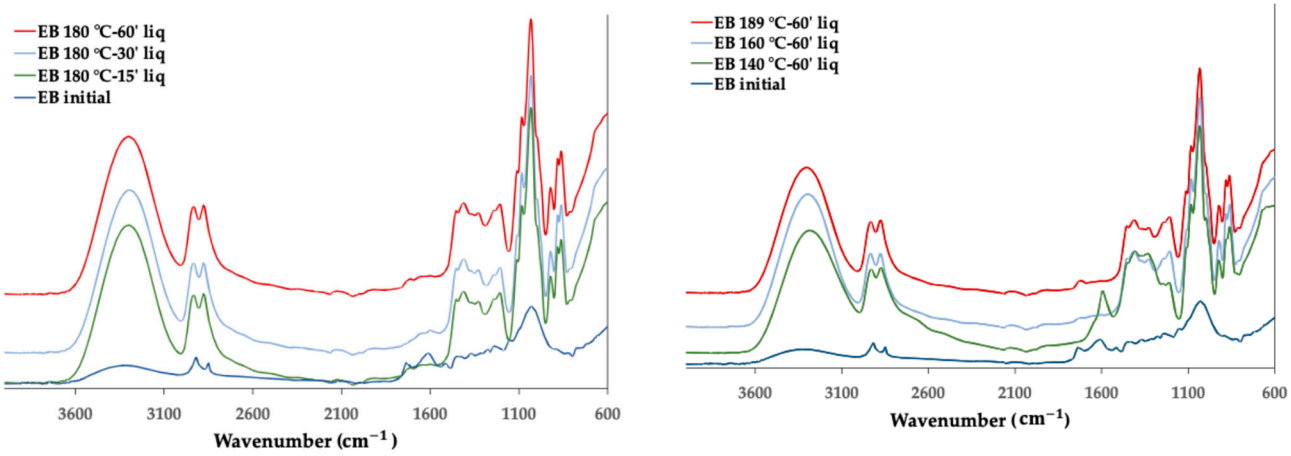

(**a**) (**b**)

Figure 3. FTIR spectra of initial EB and liquefied polyols: (**a**) With different liquefaction time; (**b**) With different liquefaction temperature.

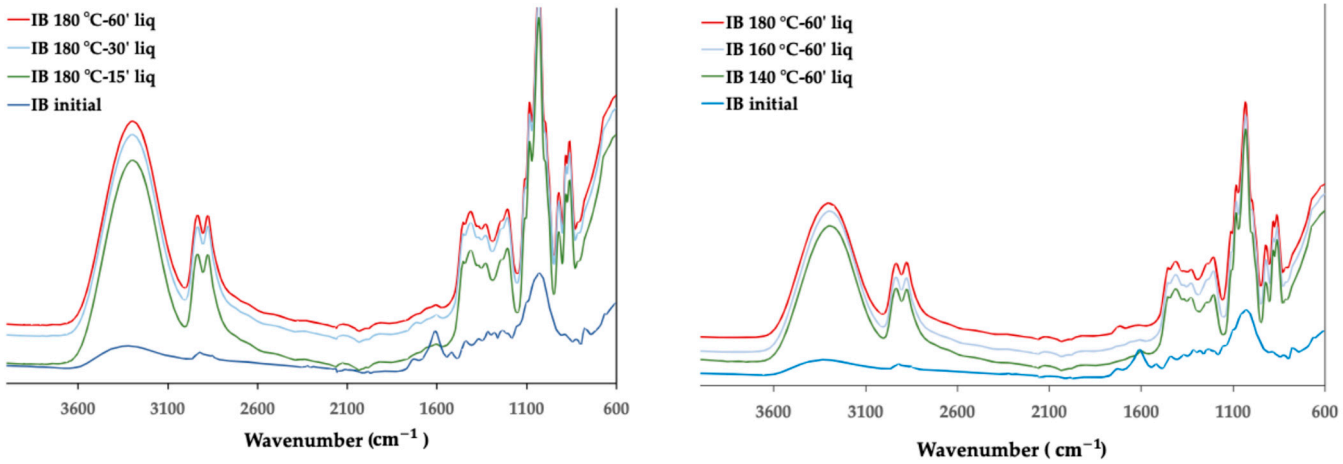

(**a**) (**b**)

Figure 4. FTIR spectra of initial IB and liquefied polyols: (**a**) With different liquefaction time; (**b**) With different liquefaction temperature.

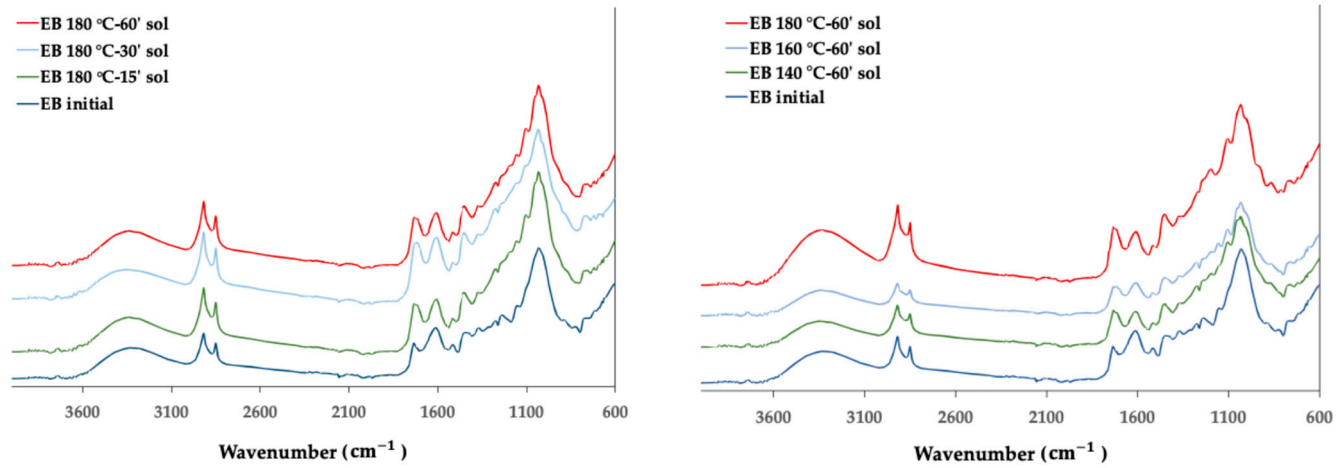

(**a**) (**b**)

Figure 5. FTIR spectra of initial EB and solid residues after liquefaction: (**a**) With different liquefaction time; (**b**) With different liquefaction temperature.

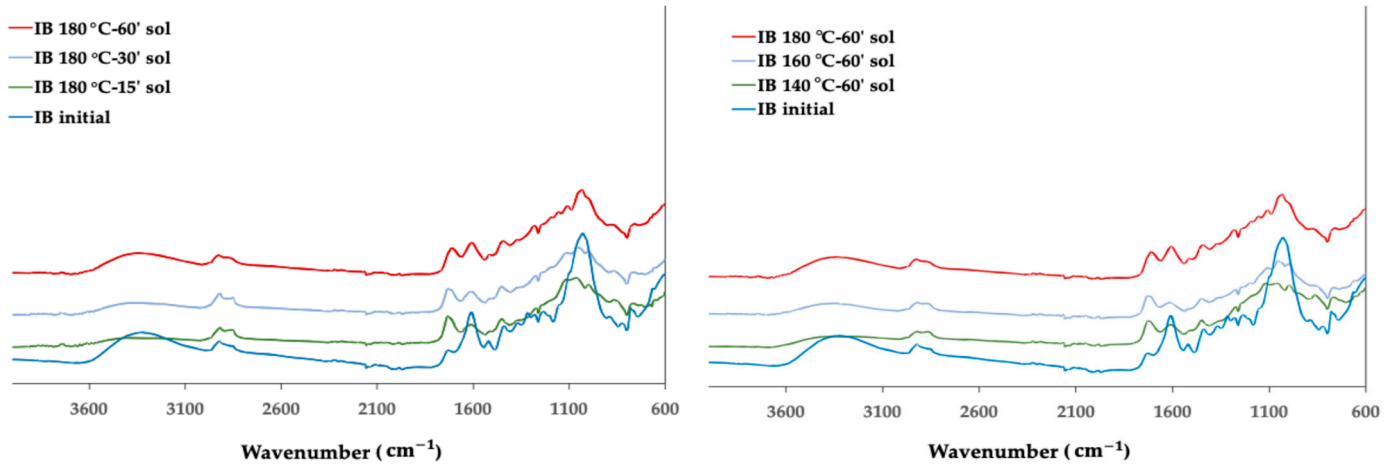

Figure 6. FTIR spectra of initial IB and solid residues after liquefaction: (**a**) With different liquefaction time; (**b**) With different liquefaction temperature.

All liquefied materials exhibit a broader and intense OH stretching peak around 3400 cm^{-1}, much higher than for the initial material, even though it is known that the penetration depth of the IR light into a liquid is typically greater than in solids due to its lower refractive index and density compared to solids, resulting in stronger absorption bands in liquids. This peak is due not only to the liquefied material but also to a significant contribution from the polyalcohols (glycerol and ethylene glycol) used in the liquefaction process, as stated before [36]. The CH stretching peaks at 2915 cm^{-1} and 2850 cm^{-1}, corresponding to asymmetric and symmetric vibrations [37], increased significantly in relation to the original internal and EB, with their maxima shifting slightly to 2927 cm^{-1} and 2870 cm^{-1}. The highest peak for the liquefied barks is the one at 2870 cm^{-1}, contrary to the initial solid material, where the 2927 cm^{-1} peak is higher, which is probably due to the different absorption patterns between liquids and solids. This behavior has been observed before for other liquefied materials, for instance, cherry seeds [38] or Scotch Broom [31]. The peak at 1730 cm^{-1} (non-conjugated C=O linkages) and the band at 1600 cm^{-1} (conjugated C=O linkages and aromatic C=C-C ring stretch) are significantly reduced and narrowed. This might be due to the significant amount of polyalcohols such as ethylene glycol and glycerol that are used as solvents that increase the carbohydrate-related peaks, attenuating the lignin-related peaks. The exception is observed at 140 °C, where a pronounced peak appears at 1600 cm^{-1}. This peak may be attributed to the increased presence of phenolic extractives, which are more readily released into the liquid phase under these conditions.

There is a high increase in the fingerprint region (1500 cm^{-1} to 600 cm^{-1}) in relation to the initial material, which can also be due to the stronger absorption bands in liquids, nevertheless, there is a clear increase in the C-O stretching band with maximum at around 1030 cm^{-1} and with a shoulder at around 1090 cm^{-1} which shows the increase in carbohydrates in the liquid fraction. Noticeably, there isn't a significant difference between different temperatures (except 140 °C) and different liquefaction times which shows that there are no big differences between the FTIR spectra of the polyols obtained at different liquefaction conditions.

The spectra obtained with the solid residues after liquefaction are relatively similar to the initial solid material, especially for external bark. The main change observed in these spectra is the increase in the 1730 cm^{-1} peak in relation to the 1600 cm^{-1} peak that is observed progressively as the temperature increases. This might correspond to an increase in non-conjugated C=O in relation to conjugated. Since conjugated carbonyl linkage is directly adjacent to a double bond, often involving alternating single and double bonds, conjugated compounds are more stable than non-conjugated ones. More condensed or cross-linked lignin structures can increase the aromatic character and thus contribute to

higher absorption at this frequency; therefore, lignin in the solid residue seems to be less cross linked and to have a less condensed structure than the initial material. Another reason might be that a higher percentage of lignin has been liquefied, or the decrease of extractable phenolic compounds that are released to the liquid fraction. For internal bark, there is a significant decrease in the 1600 cm^{-1} peak followed by an increase in the band with the increase in temperature or liquefaction time. This initial decrease might be due to the solubilization of phenolic compounds such as tannins, as mentioned before.

For the highest temperature tested, there is an increase in the 1445 cm^{-1} peak, which is generally attributed to aliphatic CH_2 groups [33]. An increase at 1187 cm^{-1} is also observed. The peak at around 1030 cm^{-1} decreases but broadens, making a shoulder visible at 1086 cm^{-1}. This shoulder can be due to sulphate ion that absorbs in this range [39] and is present in sulfuric acid used in the liquefaction. Overall results seem to indicate that the solid residue has a structurally different lignin than the initial material.

Polyurethane foams were made using liquefied IB and EB polyols combined with isocyanate and using water as a blowing agent and DBTDL as a catalyst. Figure 7 illustrates the variation in compressive strength, compressive modulus, and density of foams with increasing water content for both EB- and IB-derived polyols. A higher compressive strength means the foam can sustain greater loads without deforming or collapsing. In practical terms, this is critical for applications where the foam is used for cushioning, packaging, or structural support. A higher compressive modulus means that the foam is stiffer and less likely to compress under a given load. Higher amounts of water content (blowing agent) led to lower mechanical properties, decreasing compressive strength from about 100 kPa to less than 20 kPa for the IB polyol. Compressive modulus also decreased for higher amounts of water, producing softer, more flexible polyurethane foams that are easier to compress. The reason for these decreases might be explained by the decrease in foam density, since higher amounts of blowing agent made the foam grow higher and with lower density. Overall, IB polyurethane foams are more resistant than EB foams, and this is seen by the significantly lower compressive strength and compressive modulus of the foams. Generally, polyols with higher functionality can create a more cross-linked structure, leading to higher compressive strength, which might imply that IB liquefied material has higher functionality polyols.

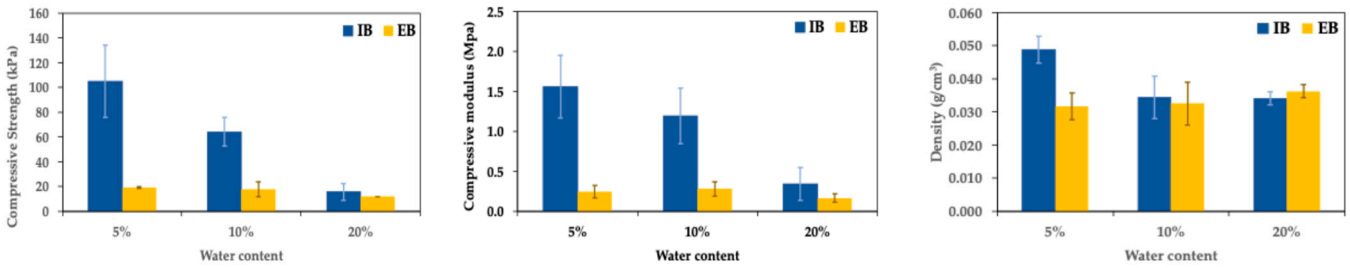

(**a**) (**b**) (**c**)

Figure 7. Variation of mechanical properties of foams with water content for IB and EB polyols: (**a**) Compressive strength; (**b**) Compressive modulus; (**c**) Density.

On the contrary, no significant differences were observed between the density of IB and EB foams, although IB foams had a generally higher density. Similar results on the variation of the mechanical strength of polyurethane foams produced with liquefied materials were presented before. For instance, foams produced from liquefied *Cytisus scoparius* also showed a decrease in both compressive strength and modulus for foams made with DBTDL catalyst, observed for both acid- and base-derived polyols [40]. The obtained values for IB polyol were in the same range as those obtained for *Cytisus scoparius*, although a little higher. The results found for IB polyol were not much different from those reported before by Li et al. [41], who reported compressive strengths of 147 kPa for 7% water content. However, most values were lower than the compressive strength of 80–150 kPa reported for

PU foams produced with polyols containing approximately 50% biomass by Yao et al. [42], or the 68–195 kPa obtained for foams made from polyols derived from various waste papers by Hu et al. [43]. The compressive strength of foams made with EB polyol with different amounts of water were all under 20 kPa, even though the density was not much lower than that observed for IB foams.

Figure 8 illustrates compressive strength and modulus for different NCO/OH ratios (isocyanate index). For an index of 0.6, compressive strength was around 45 kPa for the IB polyol and about 32 kPa for the EB polyol. As the NCO/OH ratio increased, compressive strength also increased for the IB polyol, reaching a maximum of around 60 kPa. For the EB-based polyol, compressive strength decreased. Higher isocyanate content typically improves mechanical properties due to increased hard segment content and crosslinking in the polymer network [44,45]. Nevertheless, the effect of decreasing density due to the higher expansion of the foam might overlap with the increase in hard segments. Once more, the compressive strength and compressive modulus of foams made with IB polyol presented better mechanical resistance.

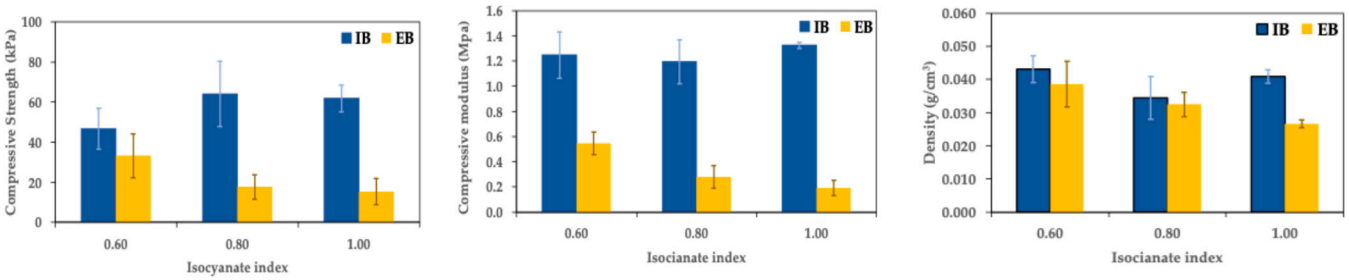

(**a**) (**b**) (**c**)

Figure 8. Variation of mechanical properties of foams with isocyanate index for IB and EB polyols: (**a**) Compressive strength; (**b**) Compressive modulus; (**c**) Density.

Figure 9 presents the effect of varying catalyst amounts on mechanical properties of IB and EB foams. For IB foams, the results on compressive strength seem to increase and decrease afterwards, but the results on the compressive modulus decrease with the amount of catalyst. For EB foams, increasing the catalyst led to a decrease in compressive strength and the compressive modulus. The decrease of mechanical properties for higher amounts of catalyst might be due to an increased rate of gas formation (blowing reaction) that can result in larger cell sizes and less uniformity in the foam structure, therefore reducing the foam's compressive strength. It is also seen that density decreases possibly due to the faster reaction trapping more gas within the foam, leading to lower overall density. Excessive amounts of catalyst have also been noted to increase the amount of side reactions [46].

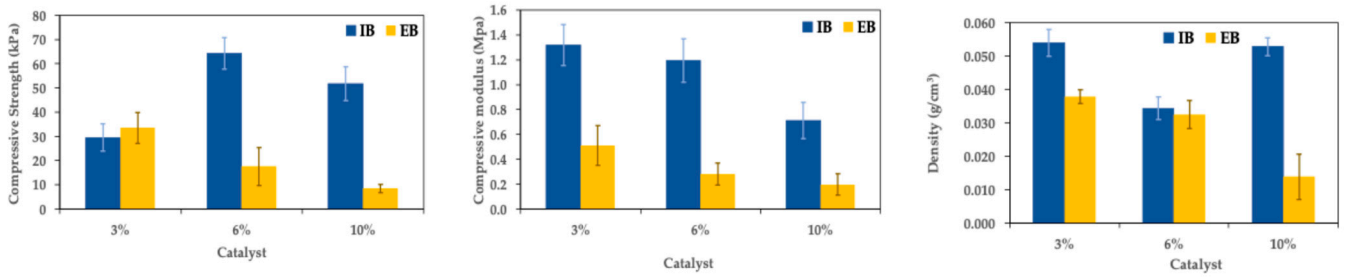

(**a**) (**b**) (**c**)

Figure 9. Variation of mechanical properties of foams with catalyst amount index for IB and EB polyols: (**a**) Compressive strength; (**b**) Compressive modulus; (**c**) Density.

4. Conclusions

The results obtained show that EB has a higher overall extractive content than IB and a higher amount of lipophilic extractives. Polysaccharides are more abundant in IB, which has higher amounts of cellulose than hemicelluloses. EB also contains more lignin compared to internal bark.

Both barks show higher liquefaction yields at increased temperatures, with internal bark liquefying slightly more efficiently due to its less condensed structure. FTIR spectra reveal significant changes post-liquefaction, indicating the breakdown of lignin and polysaccharides. Both IB and EB exhibit a notable increase in OH stretching peaks, attributed to the polyalcohols used in the liquefaction process.

Polyols derived from IB yielded stronger and more resilient foams compared to those from EB. Higher water content led to a decrease in both compressive strength and modulus, likely due to lower foam density. The mechanical properties of foams were sensitive to the NCO/OH ratio and catalyst amounts, with IB-based foams showing better compressive strength and modulus than EB-based foams, despite similar densities.

In summary, the internal bark of the strawberry tree offers superior mechanical properties for polyurethane foam production compared to external bark. This study provides insights into optimizing the liquefaction process and foam characteristics by controlling variables such as temperature, time, and catalyst content.

Future research could explore the influence of alternative catalysts and polyalcohols on the liquefaction efficiency and foam properties of IB and EB, as well as assess the environmental and economic sustainability of scaling up polyurethane foam production using bark-derived polyols.

Author Contributions: Conceptualization, L.C.-L. and B.E.; methodology, L.C.-L. and B.E.; investigation, L.C.-L., Y.D., R.L., I.D. and B.E.; resources, Y.D., R.L., I.D. and J.F.; writing—original draft preparation, L.C.-L. and B.E.; writing—review and editing, L.C.-L., R.L. and B.E.; supervision, L.C.-L. and B.E.; funding acquisition, L.C.-L. and B.E. All authors have read and agreed to the published version of the manuscript.

Funding: This research was funded by National Funds through the FCT—Foundation for Science and Technology (Proj. UIDB/00681/2020 (CERNAS) DOI: https://doi.org/10.54499/UIDB/00681/2020, accessed on 30 November 2024) and the Polytechnic University of Viseu.

Data Availability Statement: The original contributions presented in this study are included in the article, and further inquiries can be directed to the corresponding author.

Acknowledgments: This work was supported by the FCT—Foundation for Science and Technology, I.P. Furthermore, we would like to thank the CERNAS Centre and the Polytechnic Institute of Viseu for their support.

Conflicts of Interest: The authors declare no conflicts of interest.

References

1. Torres, J.A.; Valle, F.; Pinto, C.; García-Fuentes, A.; Salazar, C.; Cano, E. *Arbutus unedo* L. Communities in Southern Iberian Peninsula Mountains. *Plant Ecol.* **2002**, *160*, 207–223. [CrossRef]
2. Martins, J.; Pinto, G.; Canhoto, J. Biotechnology of the Multipurpose Tree Species Arbutus Unedo: A Review. *J. For. Res.* **2022**, *33*, 377–390. [CrossRef]
3. Miguel, M.; Faleiro, M.; Guerreiro, A.; Antunes, M. *Arbutus unedo* L.: Chemical and Biological Properties. *Molecules* **2014**, *19*, 15799–15823. [CrossRef] [PubMed]
4. Gomes, F.; Simões, M.; Lopes, M.L.; Canhoto, J.M. Effect of Plant Growth Regulators and Genotype on the Micropropagation of Adult Trees of *Arbutus unedo* L. (Strawberry Tree). *New Biotechnol.* **2010**, *27*, 882–892. [CrossRef]
5. Dönmez, İ.E.; Hemming, J.; Willför, S. Bark Extractives and Suberin Monomers from *Arbutus andrachne* and *Platanus orientalis*. *BioResources* **2016**, *11*, 2809–2819. [CrossRef]
6. Aquino, F.R.; Reyes, R.F.; Quiñones, J.G.R.; García, W.S.; Mota, M.E.S.; Reyes, H.H.E. Development and validation of an analytical method for condensed tannin extracts obtained from the bark of four tree species using HPLC. *Wood Res.* **2021**, *66*, 171–182. [CrossRef]

7. Mateus, M.M.; Guerreiro, D.; Ferreira, O.; Bordado, J.C.; dos Santos, R.G. Heuristic Analysis of Eucalyptus Globulus Bark Depolymerization via Acid-Liquefaction. *Cellulose* **2017**, *24*, 659–668. [CrossRef]
8. D'Souza, J.; Wong, S.Z.; Camargo, R.; Yan, N. Solvolytic Liquefaction of Bark: Understanding the Role of Polyhydric Alcohols and Organic Solvents on Polyol Characteristics. *ACS Sustain. Chem. Eng.* **2015**, *4*, 851–861. [CrossRef]
9. Fernandes, A.; Cruz-Lopes, L.; Dulyanska, Y.; Domingos, I.; Ferreira, J.; Evtuguin, D.; Esteves, B. Eco Valorization of Eucalyptus Globulus Bark and Branches through Liquefaction. *Appl. Sci.* **2022**, *12*, 3775. [CrossRef]
10. Gadhave, R.V.; Mahanwar, P.A.; Gadekar, P.T. Bio-Renewable Sources for Synthesis of Eco-Friendly Polyurethane Adhesives—Review. *Open J. Polym. Chem.* **2017**, *7*, 57–75. [CrossRef]
11. Lee, W.; Lin, M. Preparation and Application of Polyurethane Adhesives Made from Polyhydric Alcohol Liquefied Taiwan Acacia and China Fir. *J. Appl. Polym. Sci.* **2008**, *109*, 23–31. [CrossRef]
12. Lee, W.-J.; Kuo, E.-S.; Chao, C.-Y.; Kao, Y.-P. Properties of Polyurethane (PUR) Films Prepared from Liquefied Wood (LW) and Ethylene Glycol (EG). *Holzforschung* **2014**, *69*, 547–554. [CrossRef]
13. Barbosa, K.T.; Fuentes Da Silva, S.H.; Magalhães, W.L.E.; Amico, S.C.; Delucis, R.d.A. Acid-Catalyzed Kraft Lignin Liquefaction for Producing Polyols and Polyurethane Foams. *J. Wood Chem. Technol.* **2024**, *44*, 9–21. [CrossRef]
14. Cinelli, P.; Anguillesi, I.; Lazzeri, A. Green Synthesis of Flexible Polyurethane Foams from Liquefied Lignin. *Eur. Polym. J.* **2013**, *49*, 1174–1184. [CrossRef]
15. da Silva, S.H.F.; Egüés, I.; Labidi, J. Liquefaction of Kraft Lignin Using Polyhydric Alcohols and Organic Acids as Catalysts for Sustainable Polyols Production. *Ind. Crops Prod.* **2019**, *137*, 687–693. [CrossRef]
16. Yona, A.M.C.; Budija, F.; Kričej, B.; Kutnar, A.; Pavlič, M.; Pori, P.; Tavzes, Č.; Petrič, M. Production of Biomaterials from Cork: Liquefaction in Polyhydric Alcohols at Moderate Temperatures. *Ind. Crops Prod.* **2014**, *54*, 296–301. [CrossRef]
17. Esteves, B.; Cruz-Lopes, L.; Ferreira, J.; Domingos, I.; Nunes, L.; Pereira, H. Optimizing Douglas-Fir Bark Liquefaction in Mixtures of Glycerol and Polyethylene Glycol and KOH. *Holzforschung* **2018**, *72*, 25–30. [CrossRef]
18. Yamada, T.; Ono, H. Characterization of the Products Resulting from Ethylene Glycol Liquefaction of Cellulose. *J. Wood Sci.* **2001**, *47*, 458–464. [CrossRef]
19. Jasiukaitytė, E.; Kunaver, M.; Crestini, C. Lignin Behaviour during Wood Liquefaction—Characterization by Quantitative 31P, 13C NMR and Size-Exclusion Chromatography. *Catal. Today* **2010**, *156*, 23–30. [CrossRef]
20. Jasiukaitytė-Grojzdek, E.; Kunaver, M.; Crestini, C. Lignin Structural Changes During Liquefaction in Acidified Ethylene Glycol. *J. Wood Chem. Technol.* **2012**, *32*, 342–360. [CrossRef]
21. Choe, K.H.; Lee, D.S.; Seo, W.J.; Kim, W.N. Properties of Rigid Polyurethane Foams with Blowing Agents and Catalysts. *Polym. J.* **2004**, *36*, 368–373. [CrossRef]
22. Kurańska, M.; Prociak, A.; Michalowski, S.; Zawadzińska, A. The Influence of Blowing Agents Type on Foaming Process and Properties of Rigid Polyurethane Foams. *Polimery* **2018**, *63*, 672–678. [CrossRef]
23. Han, M.S.; Choi, S.J.; Kim, J.M.; Kim, Y.H.; Kim, W.N.; Lee, H.S.; Sung, J.Y. Effects of Silicone Surfactant on the Cell Size and Thermal Conductivity of Rigid Polyurethane Foams by Environmentally Friendly Blowing Agents. *Macromol. Res.* **2009**, *17*, 44–50. [CrossRef]
24. Blattmann, H.; Lauth, M.; Mülhaupt, R. Flexible and Bio-Based Nonisocyanate Polyurethane (NIPU) Foams. *Macromol. Mater. Eng.* **2016**, *301*, 944–952. [CrossRef]
25. Chen, X.; Pizzi, A.; Fredon, E.; Gerardin, C.; Zhou, X.; Zhang, B.; Du, G. Low Curing Temperature Tannin-Based Non-Isocyanate Polyurethane (NIPU) Wood Adhesives: Preparation and Properties Evaluation. *Int. J. Adhes. Adhes.* **2022**, *112*, 103001. [CrossRef]
26. Gomez-Lopez, A.; Elizalde, F.; Calvo, I.; Sardon, H. Trends in Non-Isocyanate Polyurethane (NIPU) Development. *Chem. Commun.* **2021**, *57*, 12254–12265. [CrossRef]
27. TAPPI T 211 Ash Test 525C. SGS-IPS Testing. Available online: https://ipstesting.com/find-a-test/tappi-test-methods/tappi-t-211-ash-test-525c/ (accessed on 25 November 2024).
28. TAPPI T 204 Extractives Soxhlet. SGS-IPS Testing. Available online: https://ipstesting.com/find-a-test/tappi-test-methods/tappi-t-204-extractives-soxhlet/ (accessed on 25 November 2024).
29. *TAPPI T 222 Om-02*; Acid-Insoluble Lignin in Wood and Pulp. TAPPI: Atlanta, GA, USA, 2002.
30. Browning, B.L. *Methods of Wood Chemistry. Volumes I & II*; John Wiley & Sons: New York, NY, USA, 1967.
31. Cruz-Lopes, L.; Almeida, D.; Dulyanska, Y.; Domingos, I.; Ferreira, J.; Fragata, A.; Esteves, B. Chemical Composition and Optimization of Liquefaction Parameters of Cytisus Scoparius (Broom). *Forests* **2022**, *13*, 1772. [CrossRef]
32. *ISO 844:2014*; Rigid Cellular Plastics—Determination of Compression Properties. ISO: Geneva, Switzerland, 2014.
33. Abd Hilmi, N.H.; Lodin, V.; Gilbert Jesuet, M.S.; Salim, S.; Lee, S.H.; Hori, N.; Takemura, A.; Palle, I. Producing *Eucalyptus pellita* Wood Polyol through Liquefaction for Polyurethane Film Production. *Ind. Crops Prod.* **2023**, *205*, 117431. [CrossRef]
34. Zhang, J.; Du, M.; Hu, L. Factors Influencing Polyol Liquefaction of Nut Shells of Different Camellia Species. *BioResources* **2016**, *11*, 9956–9969. [CrossRef]
35. Kobayashi, M.; Asano, T.; Kajiyama, M.; Tomita, B. Analysis on Residue Formation during Wood Liquefaction with Polyhydric Alcohol. *J. Wood Sci.* **2004**, *50*, 407–414. [CrossRef]
36. Cruz-Lopes, L.; Duarte, J.; Dulyanska, Y.; Guiné, R.P.; Esteves, B. Enhancing Liquefaction Efficiency: Exploring the Impact of Pre-Hydrolysis on Hazelnut Shell (*Corylus avellana* L.). *Materials* **2024**, *17*, 2667. [CrossRef] [PubMed]

37. Esteves, B.; Velez Marques, A.; Domingos, I.; Pereira, H. Chemical Changes of Heat Treated Pine and Eucalypt Wood Monitored by FTIR. *Maderas. Cienc. Tecnol.* **2013**, *15*, 245–258. [CrossRef]
38. Cruz-Lopes, L.; Dulyanska, Y.; Domingos, I.; Ferreira, J.; Fragata, A.; Guiné, R.; Esteves, B. Influence of Pre-Hydrolysis on the Chemical Composition of Prunus Avium Cherry Seeds. *Agronomy* **2022**, *12*, 280. [CrossRef]
39. Coates, J.P. Interpretation of Infrared Spectra, a Practical Approach. In *Encyclopedia of Analytical Chemistry*; John Wiley & Sons Ltd.: Chichester, UK, 2000; pp. 10815–10837.
40. Dulyanska, Y.; Cruz-Lopes, L.; Esteves, B.; Guiné, R.; Domingos, I. FTIR Monitoring of Polyurethane Foams Derived from Acid-Liquefied and Base-Liquefied Polyols. *Polymers* **2024**, *16*, 2214. [CrossRef] [PubMed]
41. Li, X.; Cao, H.; Zhang, Y. Structures and Physical Properties of Rigid Polyurethane Foams with Water as the Sole Blowing Agent. *Sci. China Ser. B Chem.* **2006**, *49*, 363–370. [CrossRef]
42. Yao, Y.; Yoshioka, M.; Shiraishi, N. Combined Liquefaction of Wood and Starch in a Polyethylene Glycol/Glycerin Blended Solvent. *Mokuzai Gakkaishi* **1993**, *39*, 930–938.
43. Hu, S.; Wan, C.; Li, Y. Production and Characterization of Biopolyols and Polyurethane Foams from Crude Glycerol Based Liquefaction of Soybean Straw. *Bioresour. Technol.* **2012**, *103*, 227–233. [CrossRef]
44. Hu, S.; Li, Y. Polyols and Polyurethane Foams from Base-Catalyzed Liquefaction of Lignocellulosic Biomass by Crude Glycerol: Effects of Crude Glycerol Impurities. *Ind. Crops Prod.* **2014**, *57*, 188–194. [CrossRef]
45. Yan, Y.; Pang, H.; Yang, X.; Zhang, R.; Liao, B. Preparation and Characterization of Water-blown Polyurethane Foams from Liquefied Cornstalk Polyol. *J. Appl. Polym. Sci.* **2008**, *110*, 1099–1111. [CrossRef]
46. Gu, X.; Luo, H.; Lv, S.; Chen, P. Glycolysis Recycling of Waste Polyurethane Rigid Foam Using Different Catalysts. *J. Renew. Mater.* **2021**, *9*, 1253–1266. [CrossRef]